Homogenization of quasiperiodic structures and two-scale cut-and-projection convergence

Stéphane Brule, Stefan Enoch, Sebastien Guenneau

PHYSICS LETTERS A – PERSPECTIVE ARTICLES

Emergence of Seismic Metamaterials : Current State and Future Perspectives

Stéphane Brûlé[1], Stefan Enoch[1] and Sébastien Guenneau[1]
[1] *Aix Marseille Univ, CNRS, Centrale Marseille, Institut Fresnel, Marseille, France*
52 Avenue Escadrille Normandie Niemen, 13013 Marseille
e-mail address: sebastien.guenneau@fresnel.fr

Following the advent of electromagnetic metamaterials, researchers working in wave physics have translated concepts of engineered media to acoustics, elastodynamics and diffusion processes. In elastodynamics, seismic metamaterials have emerged in the last decade for soft soils structured at the meter scale, and have been tested with full-scale experiments on holey soils. Born in the soil, seismic metamaterials have emerged from the field of tuned-resonators buried in the soil, around building's foundations or near the soil-structure interface as local seismic isolators. Forests of trees have been interpreted as above-surface resonators, and coined natural seismic metamaterials. We first review some advances made in seismic metamaterials and dress an inventory of which material parameters can be achieved and which cannot, from the effective medium theory perspective. We envision future developments of large scale auxetic metamaterials for building's foundations, above surface resonators for seismic protection and metamaterial-like transformed urbanism at the city scale.

Keywords: Seismic metamaterials; structured soils; effective medium; auxetic metamaterials; tuned-resonators; soil-structure interaction

I. INTRODUCTION

In Civil Engineering, the high density of deep foundation or ground reinforcement techniques for buildings in urban area, have led wave physicists to believe in a significant interaction of these buried structures (FIG. 1) with a certain component of the seismic signal. In the past, a few authors ([**1**] and [**2**]) obtained significant results with vibration screening in the soil itself for a local source such as industrial vibratory machines located on concrete slab for example.

Léon Brillouin (1946) emphasized that « *All waves behave in a similar way, whether they are longitudinal or transverse, elastic or electric* » [**3**]. However, to illustrate the interaction of seismic wave with structured soils, researchers had to adopt specific theoretical and original experimental approaches in particular because of the complexity of the wave propagation within the Earth's surface layers. As an examplar, in [**4**] and [**5**] we studied shielding and lensing of surface Rayleigh waves in the theoretical framework of linear elastodynamics. In this perspective article we illustrate how the wave interaction concept has been extended this last decade to seismic waves generated by earthquakes, which is a shift in paradigm in the topical subject of metamaterials, usually devoted to the control of electromagnetic waves [**6**]. A widely accepted definition of a metamaterial is that of a medium engineered to acquire one (or more than one) property not found in naturally occurring materials; these composites are usually designed using a combination of multiple elements arranged in repeating patterns, at one or multiple scales, that need to be smaller than the typical wavelength of the wave they aim to control. Clearly, this poses a technological challenge for fabrication of metamaterials in optics as the wave wavelength ranges from 350 to 700 nanometers for visible light and thus typical size of structural elements needs to be sub-wavelength. This is the reason why electromagnetic metamaterials have been mostly engineered to work for microwaves. For instance, the first electromagnetic cloak designed by Sir John Pendry at Imperial College London and his colleagues David Schurig and David Smith at Duke University has been fabricated and tested at 8.5 GHz: this is a frequency at which the electromagnetic wave wavelength is about 2.5 centimeters in vacuum, and thus small electric circuits could be used to achieve the desired cloak parameters. It seems thus fair to say that moving to the control of seismic waves shifts the challenges from high precision nano-technology to civil engineering techniques, requiring industrial machines able to structure soil in a precise manner at the meter scale.

From the standpoint of the mathematical theory of homogenization, the elementary cell of a metamaterial may contain one (or more) resonant element in order to achieve interesting dispersion and filtering effects, but its size should be much smaller than the wave wavelength. Indeed, the unusual effective properties of metamaterials arise from averaging processes mathematically justified by limiting processes requiring a small positive parameter, usually the ratio of elementary cell size by wavelength, to tend to zero. In practice, elementary cells of fabricated metamaterials are at least three times smaller than the wave wavelength. In such a sub-wavelength regime, metamaterials can block, absorb, enhance, bend and reflect waves in ways that go beyond what is possible with conventional materials [**6**].

The plan of the article is as follows: after this introductory part, a second section is concerned with an

overview of photonic, phononic, platonic crystals and their links to seismic metamaterials ; a third section on wave propagation in earth superficial layers ; the fourth section is at the core of the article and reviews of major scientific advances in earthquake engineering and soil structure interaction thanks to the concept of seismic metamaterials (SM) ; the fifth section then lists the different kinds of SM ; the sixth section looks at the bigger picture of transformation urbanism ; finally, the seventh section concludes the article and presents further perspectives on seismic metamaterials.

II. OVERVIEW OF PHOTONIC, PHONONIC, AND PLATONIC CRYSTALS AND THEIR LINKS TO SEISMIC METAMATERIALS

In 1987, the groups of E. Yablonovitch and S. John reported the discovery of stop band structures for light ([**7**] and [**8**]). Photonic crystals (PCs) have, since then, found numerous applications ranging from nearly perfect mirrors for incident waves whose frequencies are in stop bands of the PCs, to high-q cavities for PCs with structural defects [**9**], and waveguides with line defects. Strikingly, PCs can be made of bare glass periodically structured with small holes on the order of a few hundredths of nanometers that make it possible to reflect visible light as perfect mirrors or even to trap light in a defect within the glass. It is thus possible to design a cage for light with bare glass!

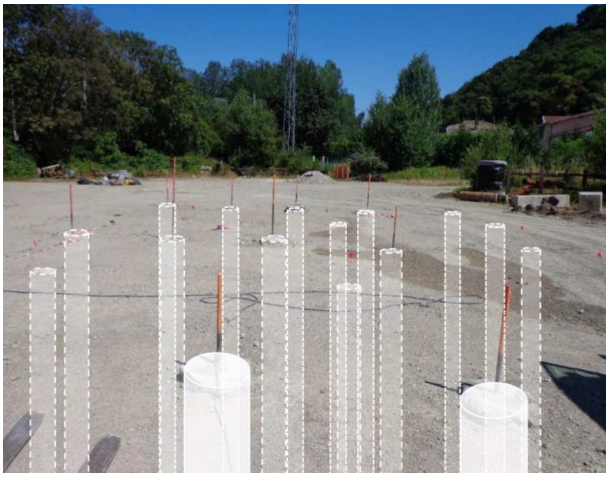

FIG. 1. Principle of artificial structured soil made of a mesh of cement columns (shown in transparency) clamped to a substratum.

The occurrence of stop bands in PCs also leads to anomalous dispersion whereby dispersion curves can have a negative or vanishing group velocity. Dynamic artificial anisotropy, also known as all-angle-negative-refraction ([**10**] to [**13**]), allows for focusing effects through a finite PC slab thanks to ray trajectories according to inverted Snell-Descartes laws of refraction, as envisioned in the 1968 paper of V. Veselago [**14**]. With the advent of electromagnetic metamaterials ([**15**] and [**16**]), J. Pendry pointed out that the image through the Veselago lens can be deeply subwavelength [**17**], and exciting effects such as simultaneously negative phase and group velocity of light [**18**], invisibility cloaks [**19**] and tailored radiation phase pattern in epsilon near zero metamaterials were demonstrated [**20**] and [**21**]. One of the attractions of platonic crystals, which are the elastic plate analogue of photonic and phononic crystals, is that much of their physics can be translated into platonics.

There are mathematical subtleties in the analysis, and numerics, of the scattering of flexural waves [**22**] in elastic plates owing to the fourth-order derivatives in the plate equations, versus the usual second-order derivatives for the wave equation of optics, involved in the governing equations; even waves propagating within a perfect plate display marked differences compared to those of the wave equation as they are not dispersionless. Nonetheless, drawing parallels between platonics and photonics helps to achieve similar effects to those observed in electromagnetic metamaterials, such as the time dependent subwavelength resolution through a platonic flat lens [**23**].

Actually, a research paper on phononic crystals provided numerical and experimental evidence of filtering effect for surface Rayleigh waves at MHz frequencies in a structured block of marble back in 1995 [**24**] and ten years ago subwavelength focusing properties [**25**] of acoustic waves via negative refraction have been achieved thanks to plasmon-like modes at the interfaces of a slab PC lens.

Localized resonant structures for elastic waves propagating within three-dimensional cubic arrays of thin coated spheres [**26**] and fluid filled Helmholtz resonators [**27**] paved the way towards acoustic analogues of electromagnetic metamaterials ([**28**] and [**29**]), including elastic cloaks ([**30**] to [**32**]). The control of elastic wave trajectories in thin plates was reported numerically [**33**] and experimentally in 2012 [**4**] and extended to the realm of surface seismic waves in civil engineering applications in 2014 [**5**]. Building upon analogies between the physics of flexural waves in structured plates and Rayleigh waves in structured soils to control surface seismic wave trajectories is not an incremental step. In order to achieve this goal, we had to solve conceptual and technological challenges. To name only a few, the duraluminium plate used in [**4**] is a homogeneous isotropic medium with simple geometric and elastic parameters, while the soil in [**5**] is heterogeneous and can only be ascribed some isotropic, homogeneous linear (e.g. non viscous) elastic parameters to certain extent, so its theoretical and numerical analysis requires some simplified assumption that can lead to inaccurate wave simulations. This means an experimental validation is absolutely necessary. Besides, Rayleigh waves are

generated by anthropic sources such as an explosion or a tool impact or vibration (sledge-hammer, pile driving operations, vibrating machine footing, dynamic compaction, etc.), and this makes the numerical simulations even more challenging. Fortunately, an excellent agreement was noted between theory and experiment in [**5**], and this opens an unprecedented avenue in the design of large scale phononic crystals for the control of seismic waves, coined seismic metamaterials in [**4**].

In 1968, R.D. Woods [**1**] created *in situ* tests with a 200 to 350 Hz source to show the effectiveness of isolating circular or linear empty trenches, with the same geometry, these results were compared in 1988 with numerical modeling studies provided by P.K. Banerjee [**2**].

The main thrust of this perspective article is to point out the possibility to create seismic metamaterials not only for high frequency anthropic sources but for the earthquakes' typical frequency range i.e. 0.1 to 12 Hz.

III. WAVE PROPAGATION IN EARTH SUPERFICIAL LAYERS

While the mathematical laws describing seismic waves are those of elastodynamics at least for earthquakes with a relatively low magnitude (i.e. in the framework of linear Navier equations), there are complexities and scalability issues that make the metamaterial transitions into the "solid Earth" realm a very challenging problem. Firstly, seismic waves have a wavelength of the order of tens if not hundred of meters at the frequencies relevant to civil engineering. Secondly the geological and seismological characteristics of the Earth's superficial layers of the crust drastically increase the complexity of the elastic wavefield.

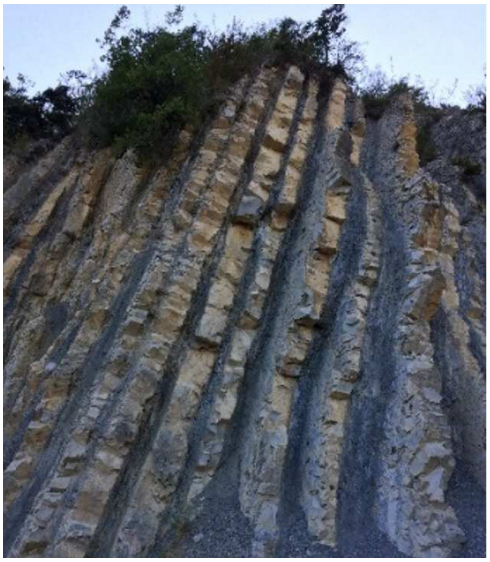

FIG. 2. Outcrop illustrating the alternation of clay (soft) – calcareous (rigid) layers reminiscent of 1D metamaterial (see FIG. 3). Serres, Drôme, France (courtesy of S.Brûlé).

Indeed, the incoming seismic signal could generate several types of surface waves and guided modes especially when waves are trapped in sedimentary basins (so-called basin resonance and seismic site effects). Finally, given the strong motion that usually accompanies seismic events, the role of the soil-metamaterial interactions and the effect played by non-linearity and attenuation remain largely unknown. We consider the case of constructions sufficiently far from the zones of tectonic faults in order to meet the conditions of applicabity of the elasticity theory.

The surface wave is the main component of wave energy in ground vibration, so researchers recently suggested the use of layered periodic structure to mitigate ground vibrations propagating in the soil [**34**]. As depicted in FIG. 3 (A) the structured soil is layered with two different engineered materials. Let us consider an alternation of layers with concrete and soil's parameters. Due to the stress-free boundary conditions at the interface between the semi-infinite substrate and air, a Rayleigh Bloch wave emerges as shown in the numerical simulation in FIG. 3 (B). Of course, one can argue that a Rayleigh wave already exists in homogeneous soil i.e. when the contrast between the two alternating layers vanishes. However, the dispersion of the Rayleigh wave in the present high-contrast layered case differs markedly from the classical Rayleigh wave as many low frequency stop bands appear below the Rayleigh 'light line' marked as a blue dotted line in the band diagram in FIG. 3(C). Similar stop bands have been observed for soils surmounted by forest of trees, and we shall come back to this in the sequel. One should note that dispersion curves above the Rayleigh 'light line' correspond to bulk (coupled shear and pressure) waves propagating within the layered soil.

Due to its periodicity, the typical cell (see Fig. 3(A)) is commonly used to analyze the dynamic characteristics of infinitely extended periodic structures. Both layers in the typical cell are assumed to be homogeneous, isotropic, and perfectly bonded at the interface. Ignoring the body force, the harmonic motion of a 2D plane strain typical cell (Eq. 1) can be drawn as follows [**35**]:

$$\frac{1}{\rho(r)}\left[\frac{\partial}{\partial x_i}\left(\lambda(r)\frac{\partial u_j}{\partial x_j}\right)+\frac{\partial}{\partial x_j}\left(\mu(r)\left(\frac{\partial u_i}{\partial x_j}+\frac{\partial u_j}{\partial x_i}\right)\right)\right]=-\omega^2 u_i^2\ (i,j=x,z) \quad (1)$$

where u, ρ, λ, and μ are the displacement, density, and two Lamé's parameters of the heterogeneous medium, respectively; r is the pointing vector and ω is the circular frequency. This equation (1) can be recast in a more compact form as an equilibrium equation $\nabla.\boldsymbol{\sigma}=\rho\omega^2 u$, where the rank-2 Cauchy stress tensor σ is linked to the rank-2 strain tensor $\boldsymbol{\varepsilon}=(\nabla u+u\nabla)/2$ via the constitutive

equation $\boldsymbol{\sigma} = C : \boldsymbol{\varepsilon}$, where the rank-4 elasticity tensor satisfies Hooke's law. The compact formulation becomes particularly useful, when one needs to model anisotropic media.

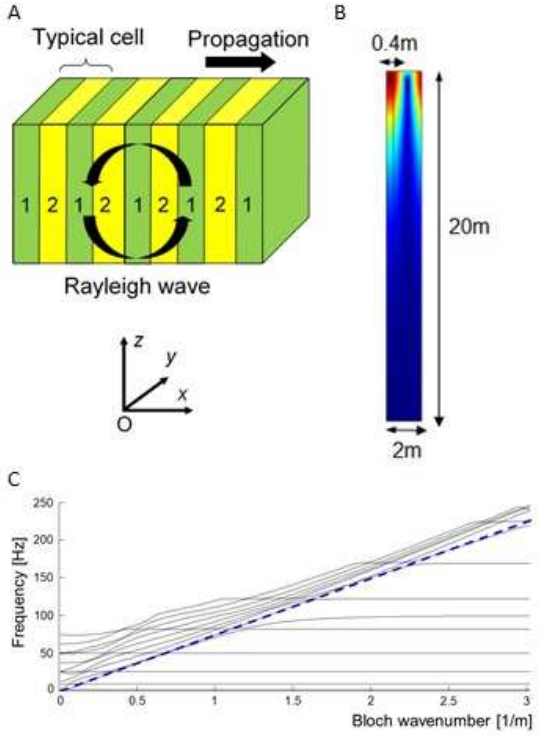

FIG. 3. (A) Schematic diagram of a vertical-layered and periodic geological structure (1D); (B-C) Simulation of a Rayleigh Bloch wave propagating within a soil (thick layer)-concrete (thin layer) periodic medium, with stress-free and clamped boundary conditions on top and bottom sides, respectively, and Floquet-Bloch conditions on vertical sides. Color scale ranges from dark blue (vanishing amplitude of displacement field) to red (maximum amplitude). Note the contrast in material parameters makes this a locally resonant structure, as can be deduced from the flat bands emerging from cut-offs in the dispersion of classical Rayleigh wave (marked as a dotted blue line).

This periodic barrier made of open trench, polyfoam in-filled trench, rubber in-filled trench or concrete panel [**34**] is effective for signal of few tens of hertz (railways vibrations, etc.). Further note that the leftmost and rightmost vertical sides of the periodic cell in Fig. 3(B) are supplied with Floquet-Bloch boundary conditions that induce a phase shift like $u_i(x+l,\mathrm{z}) = u_i(x,\mathrm{z})e^{ikl}$ where l is the array pitch and k the Bloch wavenumber that lies in the irreducible Brillouin zone $[0,\pi/l]$. It should also be noted that some surface waves akin to spoof-Love waves [**52**], which are polarized in the out-of-plane direction y, could potentially propagate in such a medium without the usual guiding sublayer, thanks to the periodicity of the substrate. Indeed, it has been theoretically established over a decade ago that the spectrum of the Helmholtz operator for the anti-plane shear waves consists of a Bloch spectrum (bulk waves) and a boundary spectrum (surface waves) [**53**].

IV. REVISITING EARTHQUAKE ENGINEERING AND SOIL-STRUCTURE INTERACTION

Most of the vibration energy affecting nearby structures is carried by Rayleigh surface waves. Earthquake Engineering is concerned with the horizontal component of bulk and surface waves [**4**].

The response of a structure to earthquake shaking is affected by interactions between three linked systems: the structure, the foundation, and the soil underlying and surrounding the foundation. Soil-structure interaction analysis evaluates the collective response of these systems subject to a specified ground motion. The terms Soil-Structure Interaction (SSI) and Soil-Foundation-Structure Interaction (SFSI) are both used to describe this effect ([**36**]).

The term free-field refers to motions that are not affected by structural vibrations or the scattering of waves at, and around, the foundation. SSI effects are absent for the theoretical condition of a rigid foundation supported on rigid soil. However, in the case of structured soils and, among them, seismic metamaterials, we are specifically looking at potential interactions with high concentration of foundations in the soil (piles, retaining walls, inclusions, etc.).

Earthquake Engineers can act in different ways for the design of structures. In most of the cases, they can directly use the input data from the local regulation which is the result of a deterministic or probabilistic analysis of the seismic hazard.

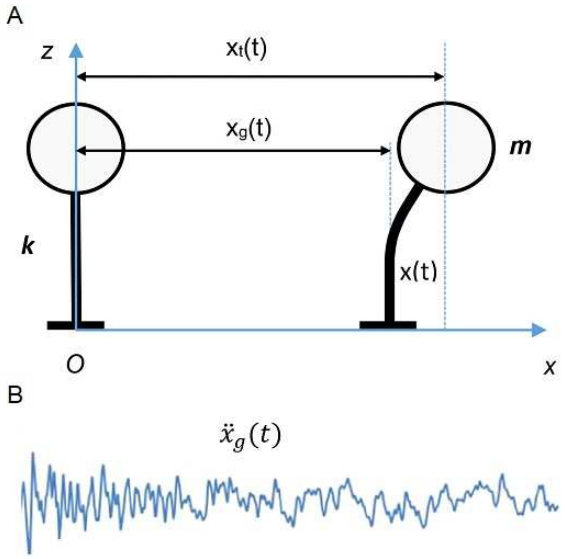

FIG. 4. (A) Principle of usual single degree of freedom oscillator (SDOFO) model for a building (From [**37**]). (B) Horizontal component of the accelerogram (generated by velocimeters), recorded at Earth's surface.

For an elastic approach of the structure, engineers usually introduce frame ductility, seismic insulators or soil-structure interaction, to reduce the pseudo-static loads applied or to improve the mechanical response of the structure.

Most of the time in earthquake engineering, the dynamic response of a building is formulated as an elastic response spectrum S(T, ξ), in acceleration S_a, velocity S_v or horizontal displacement S_d of a system (mass m, stiffness k) simplified as a single degree of freedom oscillator (SDOFO) under seismic acceleration of the soil $\ddot{x}_g(t)$.

From each seismogram, earthquake engineers point out the maximum value of acceleration, velocity or displacement, for a relative displacement x(t) in time domain, for given damping ratio ξ_0 and a fundamental period T of the structure (FIG. 4) and natural pulsation ω_0. Duhamel's integral is a way of calculating the response of linear structures x(t) which is the steady state solution, to arbitrary time-varying external perturbation $\ddot{x}_g(t)$ (Eq. 2).

$$x(t) = \frac{1}{\omega_d}\int_{\tau=0}^{\tau=t} \ddot{x}_g(\tau) e^{-\xi_0\omega_0(t-\tau)} \sin\big(\omega_d(t-\tau)\big)\, d\tau \qquad (2)$$

Here, $x_t(t)$ is the overall displacement for a visco-elastic system and $x_g(t)$ is the displacement of the soil deduced from the records of surface seismograph. Besides ω_d is the damped pulsation of the system.

Except for a few cases with full numerical modeling, the complete study of both the structure and deep foundations (piles) is complex and usually the problem is split into two cases: kinematic and inertial interactions (FIG. 5).

Kinematic interaction results from the presence of stiff foundation elements on or in soil, which causes motions at the foundation to deviate from free-field motions. Inertial interaction refers to displacements and rotations at the foundation level of a structure that result from inertia-driven forces such as base shear T and moment M.

The first research progress of this last decade in seismic metamaterials is the development of the interaction of structured soil with the seismic signal propagating in superficial Earth's layers [**38**] and then an active action on the kinematic effect described above. The second research advance is the experimental modal analysis of composite systems made of soil, piles and structures by means of numerical analysis and the confirmation of these predictions by full-scale experiments held in situ.

Interestingly, the kinematic and inertial interactions are encapsulated in some enriched linear elastodynamic model, established by the British applied mathematician John Willis over 35 years ago using some dynamic homogenization approach [Willis1981]. The eponymous equations take the form of a constitutive equation

$$< \boldsymbol{\sigma} >= C_{eff} *< \boldsymbol{\varepsilon} > + S_{eff} *< \dot{u} >, \qquad (3)$$

and two equilibrium equations

$$\nabla . < \boldsymbol{\sigma} > + \boldsymbol{f} =< \dot{p} >, \qquad (4)$$

$$< p >= S_{eff}^{\perp} *< \boldsymbol{\varepsilon} > + \rho_{eff} *< \dot{u} >. \qquad (5)$$

Here, <> denotes some ensemble average, * the time convolution, **f** the body force, p the momentum density and **s** is the Cauchy stress rank-2 tensor, $< \boldsymbol{\varepsilon} >= (\nabla < u > + < u > \nabla)/2$. Besides, C_{eff}, S_{eff} and ρ_{eff} are non-local operators (respectively rank-4, rank-3 and rank-2 tensors) depending upon the angular frequency ω. $S_{eff}^{\perp}$ is the adjoint of S_{eff}.

We shall come back to these so-called Willis equations in the sequel, since they happen to be an essential ingredient of seismic cloaks designed by performing geometric transforms in the elastodynamic equations. Before that we would like to classify the different kinds of seismic metamaterials, which have been proposed by physicists and civil and mechanical engineers in the past ten years.

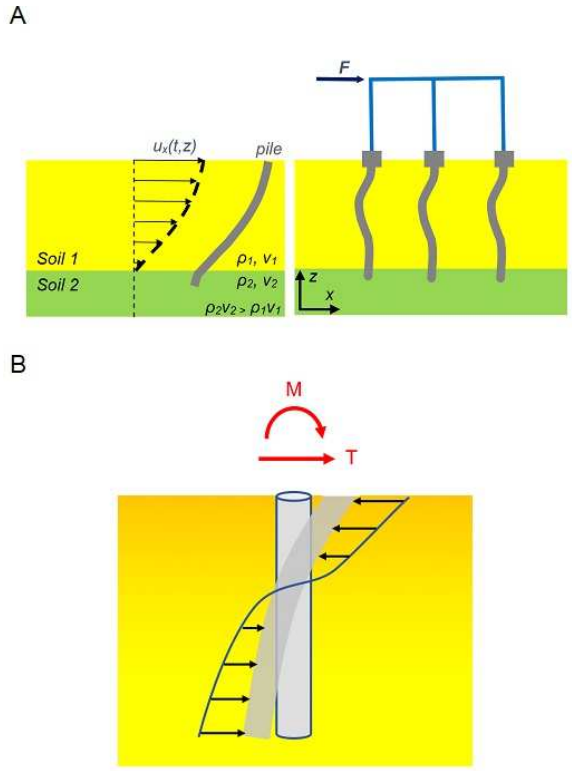

FIG. 5. (A) Earthquake Engineering for deep foundations. Kinematic interaction (left) and inertial effect (right). Inspired from [**36**]. (B) Detail of soil's reaction under inertial effect. M and T are respectively the moment and the shear load applied at the head of the pile or inclusion.

V. CATEGORIES OF SEISMIC METAMATERIALS

Even if the field of seismic metamaterials is fast growing, with a plethora of theoretical proposals that we cannot all review (some of which envision exciting developments at the frontier between surface science, which is concerned with the nanoworld, and geophysics, thereby spanning the scales [**42**]), we can identify four main types of seismic metamaterials, that have emerged after a decade of research.

Seismic Soil-Metamaterials

The first type of seismic metamaterial includes structured soils made of cylindrical voids ([**4**], [**5**] and [**40**]) or rigid inclusions ([**41**] and [**42**]). This first group in order of chronological appearance can be named "Seismic Soil-Metamaterials" or SSM (FIG. 6).

Two full-scale experiments led by the Menard company in Summer 2012 near the French cities of Grenoble [**4**] and Lyon [**5**] with cylindrical holes allowed the identification of the Bragg's effect and the distribution of energy inside the grid (FIG. 6), which can be interpreted as the consequence of an effective negative refraction index. Such a flat lens is reminiscent of what Veselago and Pendry envisioned for light.

Another effect on ground displacement is the frequency dependence of the horizontal to vertical Fourier spectra ratio when the signal passes through the lens (20 m in width, 40 m in length) made of 23 holes (2 m in diameter, 5 m in depth, triangular grid spacing 7.07 x 7.07 m). In this case, the artificial anisotropy (FIG. 7) reduces the horizontal amplification between 5 and 7 Hz [**5**]. For example, this corresponds to the frequency of the first fundamental mode of a "stiff" i.e. low-rise building (less than four floors) while a taller building is more flexible.

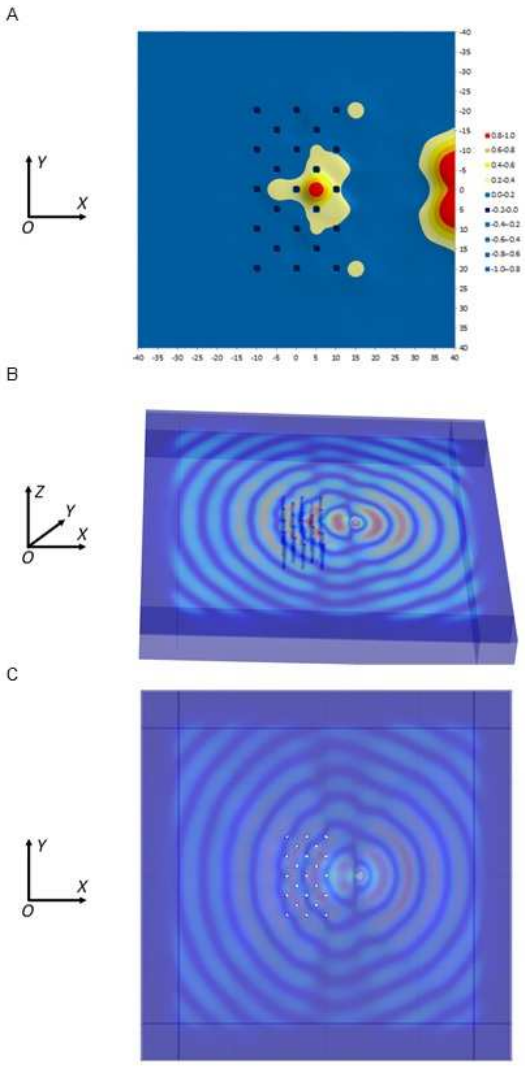

FIG. 6. (A) Snapshot illustrating the recorded energy distribution in a soil structured with 23 holes after an impact at the Earth's surface [**5**]. Source is located at (x=-40, y=0) with a mean frequency content around 8 Hz. (B) Three-dimensional simulation (comsol) of an elastic wave generated by a vertical point force pulsating at 8 Hz in front of 23 stress-free inclusions (depth 50m, diameter 2m, center-to-center spacing 7m) in a thick plate (thickness 50m) with soil parameter (Young modulus E=0.153 GPa, Poisson ratio ν=0.3, density ρ=1800 kg/m3), showing lensing effect as in (A). Color scale ranges from dark blue (vanishing amplitude of displacement field) to red (maximum amplitude). Note the perfectly matched layers that model a plate of infinite transverse dimensions. (C) Top view of the simulation exemplifying the lensing effect.

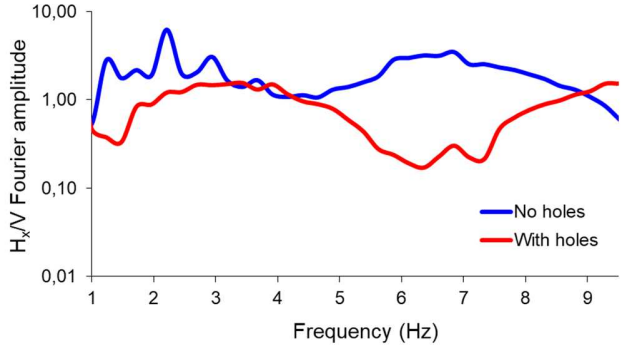

FIG. 7. Experimental test for 23 holes in the soil. Ratio of the horizontal Hx to the vertical V components of ground motion versus frequency; seismic land streamer on a soil without holes (blue solid line) and same acquisition device for holey soil (red solid line). Sensor is located at 50 m from the source location (See FIG. 8).

The theoretical dynamic response of a building (FIG. 8A) was tested with real seismogram recorded during the 2012 experimental test depicted in FIG. 5. Here, the elastic response spectrum $S_a(T, \xi)$ is calculated (Eq. 2) for the horizontal acceleration of a SDOFO under seismic acceleration of the soil $\ddot{x}_g(t)$. FIG. 8B is the graph of all the maximum values of pseudo-acceleration $a_{pseudo}(T)$. First we calculate the relative maximum displacement x(t) of the gravity center of the SDOFO. Then we define, for all $x_{max}(T)$, the pseudo-acceleration $a_{pseudo} = |\omega_0^2 x_{max}|$ of the SDOFO, with ω_0 its circular frequency for the fundamental mode

We vary the value of the structure's period and progressively draw the spectrum for the case without holes (blue line) and the case with holes (red line). The theoretical structure is located at 50 m from de source, just behind the mesh of holes. Experimental data show a bandwidth diminution for the resonance of the structure and a shift towards a higher period value for the maximum horizontal pseudo-acceleration. These results illustrate the significant change of the kinematic effect (§IV) due to the structured soil and thus, theoretically, the modification of the structure's response (i.e inertial effect).

These results are consistent with that of FIG. 7. In fact, the natural soil without holes amplifies the horizontal motion for frequencies band between 1-2 Hz and 5-7 Hz. For a ground acceleration around 1 to 2 Hz, usual buildings (5 to 10 storeys) are sensitive because they have a fundamental frequency in the same frequency range.

In the continuity of these first experiments on structured soils, a promising way to cause a modification on any seismic disturbance is to create a complete dynamic artificial anisotropy by implementing geometrical elements, full or empty, in the soil.

The physical process is the interference of waves (body or surface waves) scattered from surfaces or objects. The effects of the dynamic anisotropy are reinforced by the local resonance of implemented, which are disposed along a grid according to transformation elastodynamics ([**40**] and [**43**]) and morphing tools [**42**] that could theoretically lead to an ideal cloak detouring waves around a protected area (FIG. 9). On this occasion, and in order to explore the outstanding peculiarities of crystallography, the researchers also test motifs with five-fold symmetry such as quasi-crystals generated by a cut-and-projection method from periodic structures in higher-dimensional space [**42**].

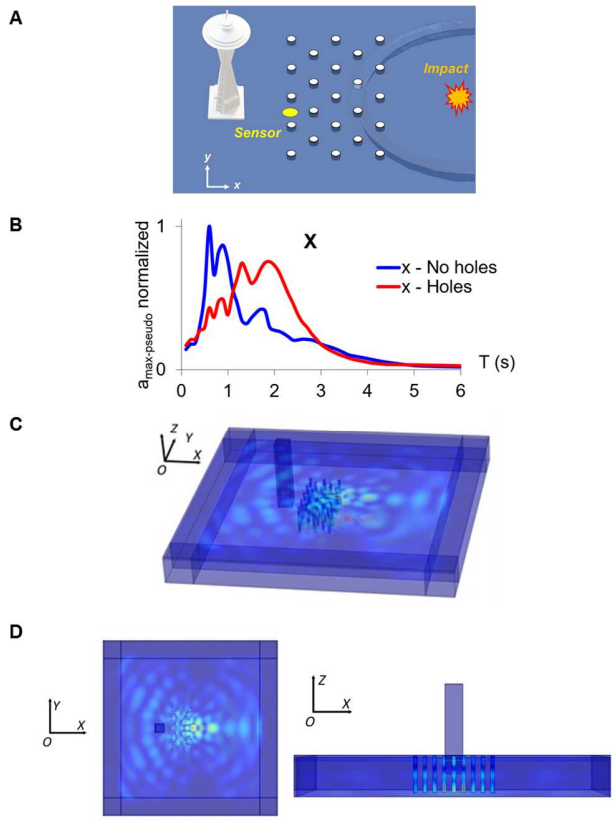

FIG. 8. Experimental test for 23 holes in the soil for theoretical studies of the dynamic response x(t) of a building modeled as a SDOFO (A). The reference sensor (yellow disk) is located behind the grid, before the SDOFO. Dynamic response calculated in relative X-horizontal maximum and normalized pseudo-acceleration versus T, the fundamental period of the SDOFO (B). The damping is $\xi_{building}$ = 0.02. (C) Three-dimensional finite element simulation for a time-harmonic source like in Fig. 6 but pulsating at 10 Hz. Note this frequency corresponds to the minimum of spectral h/v ratio in Fig. 7. (D) The side and top views of 3D simulation exemplify the vanishing displacement field amplitude in the building.

In this periodic or non-periodic media, the desired effects are total reflection (Bragg's effect), band-gaps, wave-path control via specially designed anisotropy, attenuation by energy-dissipation (e.g. heat conversion), etc.

In case of vertical columns, numerical simulations have shown zero frequency stop-bands that only exist in the limit of columns of concrete clamped at their base to the bedrock. In a realistic configuration of a sedimentary basin 15m deep we observe a zero frequency stop-band covering a broad frequency range of 0–30 Hz [**41**].

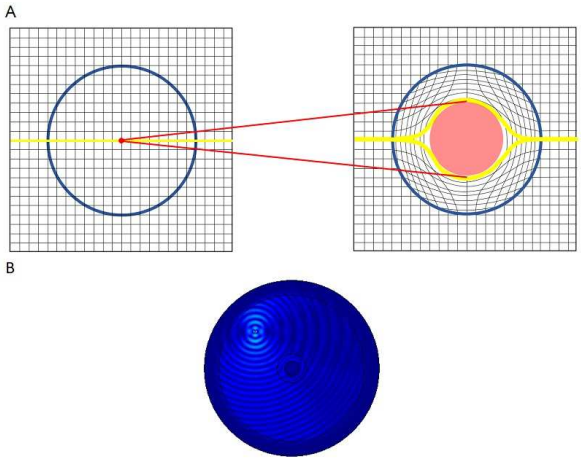

FIG. 9. Illustration of the transformation of a disk into a ring (inspired by [**39**]) from virtual (A) to physical (B) space; (C) Simulation (comsol) of an elastic wave generated by a point force detoured by a seismic cloak. Color scale ranges from dark blue (vanishing amplitude of displacement field) to red (maximum amplitude). Note the perfectly matched concentric layer that models the infinite outer medium.

Buried Mass-Resonators

The second type of seismic metamaterial consists of resonators buried in the soil (FIG. 10) in the spirit of tuned-mass dampers (TMD) like those placed atop of skyscrapers. We call this group "Buried Mass-Resonators" (BMR).

We do not consider here the resonators not buried or forming part of the structure. We consider these concepts to be in line with the technologies of seismic isolators.

TMD or BMR is a device consisting of a mass, a spring, and a damper that is attached to a structure for the TMD or in the soil for BMR, in order to respectively reduce the dynamic response of the structure or the soil. The frequency of the damper, or the set of oscillators, is tuned to a particular structural frequency so that when that frequency is excited, the damper will resonate out of phase with the structural motion. The energy is dissipated by the damper inertia force acting on the structure.

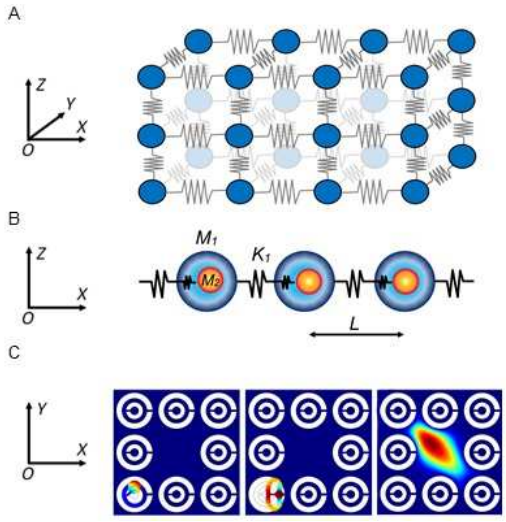

FIG. 10. Top (A), modeling a 3D isotropic elastic solid. Middle (B), modeling the propagation medium consisting of a chain of oscillators with nested masses (1D). Illustration of a single mass m_1 with an imbricated mass m_2. The set is equivalent to a unique mass m_{eff}. The system is under a dynamic loading F(t) in y direction. From [**44**] and [**45**]. Bottom (C), numerical simulations for Floquet-Bloch in-plane elastic waves propagating within a doubly periodic array of supercells (sidelength 6 m) of eight split ring resonators (SRRs) (stress free inclusions in a bulk with soil parameters like in Fig. 6) with a defect, which are the continuous counterpart of discrete models in (A,B). Color scale ranges from dark blue (vanishing amplitude of displacement field) to red (maximum amplitude). This metamaterial creates low frequency stop bands (in the range [1, 10] Hz) associated with localized bending and longitudinal modes within any one of the SRRs, and the defect in the center of the supercell is associated with a defect mode that sits within the stop bands.

Interestingly, some authors [**46**] propose using cross-shaped, hollow and locally resonant (with rubber, steel and concrete), cylinders to attenuate both Rayleigh and bulk waves in the 1-10 Hz frequency range. Although this metamaterial seems difficult to implement at a reasonable cost with currently available civil engineering techniques, it certainly opens an interesting route for seismic wave protection.

Unfortunately, the main drawback of this type of locally resonant structure is the difficulty in obtaining very large efficient stop bands; there is always a trade-off between the relative bandwidth and the efficiency of the attenuation, which is directly linked to the quality factor of the resonators. The frequency bandwidth of wave protection can be enlarged by considering arrays of resonant cylinders with different eigenfrequency for two-dimensional stop-bands [**47**], or cubic arrays of resonant spheres [**48**] for 3D stop-bands, but such mechanical metamaterials would be hard to implement at the civil engineering scale. Buried isochronous mechanical oscillators based on spheres rolling over cycloidal trajectories in cavities buried in soil have been also envisaged to filter the shear waves of an earthquake [**49**]. This proposal makes use of analogies with spring-mass systems.

Above-Surface Resonators

The third type of seismic metamaterial consists of sets of Above-Surface Resonators (ASR), typically, but not exclusively, these are forests of trees.

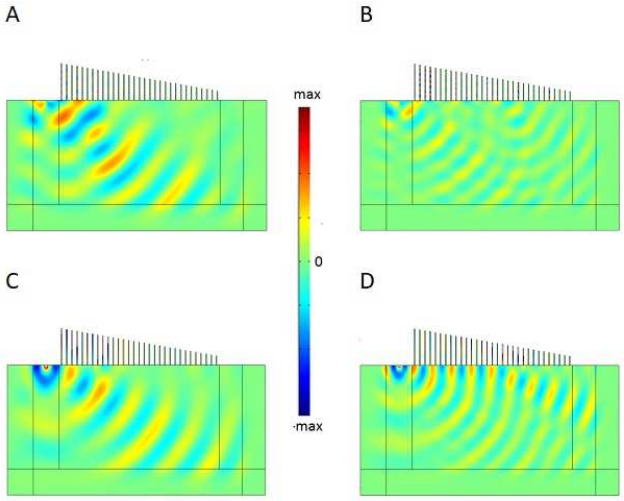

FIG. 11. Two-dimensional in-plane elastodynamic simulation of a Rayleigh wave that propagates at a frequency 70 Hz (A,C) and 120 Hz (B,D) in a forest of trees of decreasing height (14m to 4m) and same diameter (0.3m) atop a soil substrate with elastic parameters like in Fig. 6, which is converted into a downward propagating shear wave by a tree whose longitudinal resonance corresponds to a stop band for the Rayleigh wave at 70 Hz (A,C) and 120 Hz (B,D). Note the perfectly matched layers on bottom, left and right sides as well as corners to avoid reflection on computational domain boundary. Color scale ranges from dark blue (largest negative value of real part of horizontal A,B and vertical B,D displacement field) to red (largest positive value of real part of horizontal A,B and vertical B,D displacement field).

A complementary approach to buried inertial resonators, employed in [**50**, **51**] is to draw upon the metamaterials literature that utilizes subwavelength resonators arranged, in this case, upon the surface of an elastic half-space; this results in surface Rayleigh wave to bulk shear wave conversion, see Fig. 11, and surface wave filters with band-gaps but again at higher frequency than those required for seismic protection. Note that if one places the source on the right-hand side of the forest in Fig. 11, the surface wave is simply back reflected by one of the trees, and no longer converted into a bulk wave. This strongly asymmetric behavior is reminiscent of non-reciprocal media, see [**50**,

51] for more details. Care needs to be taken with the implementation of such a metawedge as depending upon the incidence of the incoming wave, it might be deleterious for building located on the wrong side of the forest, for instance in a urban environment. Nonetheless, if implemented thoughtfully, this approach might be useful for attenuation of ground vibration caused by human activity such as traffic.

This recent research on metamaterials has also spurred renewed interest in dynamic homogenization techniques with higher order corrections to asymptotic expansions, which has been notably applied to conversion of Love waves in forests of trees [**52**]. This topic is however not developed in this review paper as this research is still in its infancy. The underlying issue being how to design, by means of dynamic effective properties (mass density, etc.), an inhomogeneous medium so that it responds in a given manner (enhanced absorption, total transmission, or various patterns of scattering) to a wavelike solicitation. Interestingly, a spring-mass model has been recently proposed as Above-Surface-Resonators in order to achieve some design of gradient index lenses for Love waves [**54**]. Therefore, it seems that there is currently a growing interest in the control of Love waves within structured soils.

In the same spirit of Above-Surface-Resonators but on a smaller model, Wirgin [**55**] defined the applicability of effective medium parameter for a structure composed of a 1D periodic set of identical, perfectly-rigid rectangular blocks whose heights are h = 0.00475 m and whose spatial period is 0.004 m. The model has been numerically tested and the solicitation was a homogeneous acoustic plane wave (tens of kHz).

Auxetic materials

The fourth type of seismic metamaterials is based on extreme properties of structured media such as auxetic metamaterials, characterized by their negative Poisson's ratio ν and buried in the soil [**61**] bring bandgaps at frequencies compatible with seismic waves when they are designed appropriately. As a reminder, Poisson's ratio is the ratio of transverse contraction strain to longitudinal extension strain in a stretched bar. Since most common materials become thinner in cross section when stretched, their Poisson's ratio is positive and so negative Poisson ratio materials are unusual. The typical bow-tie element is designed to achieve tunable elastic stop bands for seismic waves, see Fig. 12.

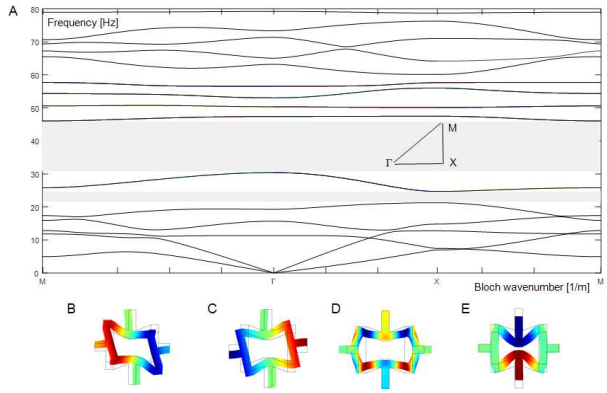

FIG. 12. Two-dimensional finite element simulation of in-plane elastic band diagram (frequency in hertz versus projection of Bloch wavevector describing the first Brillouin zone ΓXM, with Γ=(0,0), X=(π/10,0) and =(π /10, π /10)) for a periodic cell of sidelength 10m consisting of concrete beams forming an auxetic metamaterial (A). One can see two stop bands highlighted by a grey area. The edges of the lower (resp. upper) stop band are associated with motion of beams like in B, C, (res. D, E). See [**61**] for three-dimensional computations and an interpretation in terms of effective elastic parameters, as well as [**62**] for small-scale experiments confirming the theoretical proposal of tunable low frequency stop bands in [**61**].

A remaining avenue to be explored is the use of these auxetic materials, not only for the foundations but in some parts of the buildings themselves.

Other dissipative structures

By another way but with the aim of reducing the effect of the waves on the structure, recent research on gyrobeams implemented in the structure itself [**56**] has opened a new perspective on chiral metamaterial design and in a wide range of applications in earthquake wave filtering. It has been demonstrated that the role of gyrobeams is primarily to create low-frequency 'energy sinks', in which waves generated by external excitations are channelled. As a consequence, energy is diverted away from the main structure, which undergoes smaller displacements and smaller stresses.

VI. METAMATERIAL-LIKE TRANSFORMED URBANISM

In the further development, one can conceive that modern cities with their buildings can behave like a group of Above-Surface Resonators [**37**]. Indeed, when viewed from the sky, the urban fabric pattern appears similar to the geometry of structured devices as metamaterials. Visionary research in the late 1980s [**57** – **60**] based on the interaction of big cities with seismic signals and more recent studies on

seismic metamaterials, has generated interest in exploring the multiple interaction effects of seismic waves in the ground and the local resonances of both buried pillars and buildings.

Techniques from transformational optics applied to urbanism have been theoretically validated by numerical experiments to envisage some metacity-cloak like in Fig. 13 (C), (D). The essence of this transformed urbanism is as follows: the distribution of buildings (made of concrete) in this seismic cloak which is 1 km in diameter mimics the spatially varying refractive index of a conformal invisibility cloak. In this metacity-cloak design building's height ranges from 10 m to 100 m, and buildings are partially buried in the soil (with a soil depth of 40 m).

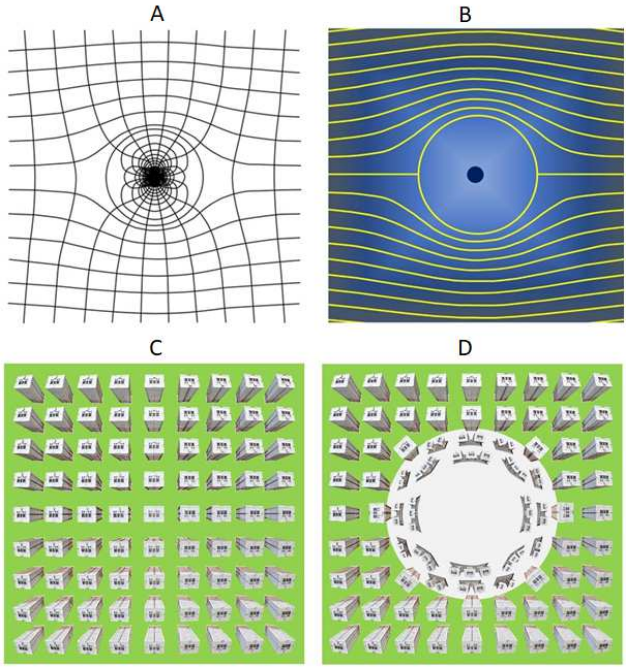

FIG. 13. Concept of Metacity cloak based upon transformation urbanism using a conformal mapping: The curved coordinate grid in (A) is the inverse map $z(w) = \frac{1}{2}\left(w \pm \sqrt{w^2 - 4a^2}\right)$ of the w coordinates, where a is a given constant characterizing the spatial extension of the cloak, approaching a straight rectangular grid at infinity, as first proposed in optics in [**71**]. As a feature of conformal maps, the right angles between the coordinate lines are preserved. (B) Surface seismic ray propagation in the cloaking device. The rays shown in yellow are solutions of Eq. (7). The brightness of the blue background indicates the transformed spectral parameter profile in Eq. (8). The curved lines in (A) correspond to the shape of avenues or main roads in the Metacity cloak, and blocks of buildings should be organized in each cell of the grid in such that density and height of buildings is distributed according to Eq. (8). (C) and (D) show a city map before (C) and after (D) conformal mapping.

Following the proposal of Leonhardt for an invisibility cloak via conformal mapping in the Helmholtz equation [**71**], which is a good approximation of Maxwell's equations in the ray optics limit, we propose to apply the same scheme to the Kirchhoff-Love (KL) biharmonic equation for flexural waves in plates,

$$\left(\left(\frac{\partial}{\partial x}\right)^2 + \left(\frac{\partial}{\partial y}\right)^2 + \beta_0^2\right)\left(\left(\frac{\partial}{\partial x}\right)^2 + \left(\frac{\partial}{\partial y}\right)^2 - \beta_0^2\right)u_3 = 0 \quad (6)$$

where the spectral parameter $\beta_0^4 = h\frac{\rho\omega^2}{D}$, with h the plate thickness, ρ, its density, D is flexural rigidity and ω the wave frequency.

Large scale experiments in [**4**] have shown that this KL equation can be used as a simplified model for surface seismic waves. After transform the KL equation looks like

$$\left(4\left(\frac{\partial}{\partial z}\right)^*\left(\frac{\partial}{\partial z}\right) + \beta^2\right)\left(4\left(\frac{\partial}{\partial z}\right)^*\left(\frac{\partial}{\partial z}\right) - \beta^2\right)u_3 = 0 \ (7)$$

We note that the Laplace operator is such that $\left(\frac{\partial}{\partial x}\right)^2 + \left(\frac{\partial}{\partial y}\right)^2 = 4\left(\frac{\partial}{\partial z}\right)^*\left(\frac{\partial}{\partial z}\right)$ with z=x+iy and * denotes the complex conjugation.

Let us introduce new coordinates w described by an analytic function w(z) that does not depend on z*, and its inverse map z(w) : $w(z) = z + \frac{a}{z^2}, z(w) = \frac{1}{2}\left(w \pm \sqrt{w^2 - 4a^2}\right)$, as shown in Figure 13(A). The constant a characterizes the spatial extension of the cloak. Such functions define conformal maps that preserve the angles between the coordinate lines. Because $\left(\frac{\partial}{\partial z}\right)^*\left(\frac{\partial}{\partial z}\right) = \left|\frac{dw}{dz}\right|^2\left(\frac{\partial}{\partial w}\right)^*\left(\frac{\partial}{\partial w}\right)$, we obtain in w space a KL equation with the transformed spectral parameter (akin to the refractive-index in optics) profile β defined as

$$\beta(z) = \left|1 - \frac{a^2}{z^2}\right|\beta_0, \quad (8)$$

where a characterizes the radius of the cloak. The spatially varying β can be obtained through a variation of the plate thickness, its density and its flexural rigidity.

For seismic wave applications, if one would like to achieve a Metacity cloak self-protecting its center from surface seismic waves with trajectories as in Figure 13(B), the urban map should be planed with the soil density and building heights to achieve the required profile for β as in Eq. (8). This can be done for instance using some soil compaction techniques, and the corresponding transformed urbanism map is shown in Figure 13(D).

VII. CONCLUDING REMARKS

The last decade has been marked by the emergence of mechanical metamaterials [**6**] including seismic metamaterials. Well beyond the important scientific and technological advances in the field of structured soils, the concepts of superstructures "dynamically active" under seismic stress and interacting with the supporting soils (soil kinematic effect) and its neighbors is clearly highlighted.

In this perspective article, we have stressed in Fig. 7 that more than the striking lensing effect for Rayleigh waves already reported in [**5**], there is a change in the effective ellipticity of ground motion thanks to the array of boreholes. This could be a key advantage for buildings's seismic design, since buildings are mainly sensitive to the horizontal component of the ground motion **[36]**.

One of many objectives is detouring surface seismic waves around protected areas, and this can be achieved via the metacity and seismic cloaks concepts like in Fig. 13 & 14. Note that our two-dimensional in-plane elastodynamic computations of the seismic cloak designed using a direct geometric transform in Fig. 14, first proposed in [**42**] motivate further analysis of the mechanical cloak of Wegener's group [**63**]. Indeed, it would be interesting to check whether the latter works beyond the quasi-static regime, and in this case it would make a good candidate for a seismic cloak.

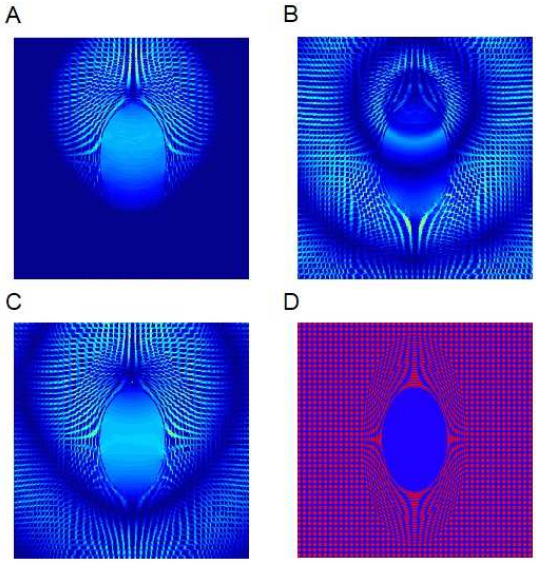

FIG. 14. Tow-dimensional finite-time-domain simulation (SIMSONIC freeware) of an in-plane seismic wave of central frequency 10 Hz incident upon an elliptical cloak consisting of columns of concrete buried in soft soil (with parameters close to soil undergoing liquefaction i.e. with a density of $10^3 kgm^{-3}$ and a Poisson ratio close to 0.5) at three consecutive time-steps of 100ms (A), 150ms (B) and 200ms (C). This seismic cloak which is viewed from the sky is deduced from a mapping of a square grid of columns 0.5m in diameter, with a center-to-center spacing of 1.5m, onto a deformed grid (D), see [42] for more details.

Tools for exploring the design of structured soil configurations have been developed ([**41**], [**42**], [**46**]) and first full-scale experimental tests have shown the influence of these buried structures on the propagation of surface waves ([**4**], [**5**]). Three types of seismic metamaterials are distinguished: "Seismic Soil-Metamaterials" (SSM), "Buried Mass-Resonators" (BMR) and Above-Surface Resonators (ASR). At this stage, such mechanical metamaterials as BMR would be hard to implement at the civil engineering scale, except for frequency vibration (>30 Hz) generated by human activities.

A few authors have suggested an intermediate concept between pure seismic isolators and devices located at foundation level. The device is then designed with the metamaterials tools [**64, 65**].

There are good prospects for SSM because the process is capable of producing large quantities of elements in the soil, and ASR, especially if their effects can be coupled.

In parallel, new possibilities to dissipate the seismic energy in the superstructures themselves are emerging thanks to the contributions of auxetic materials [**61,62**] and metamaterials [**64-66**].

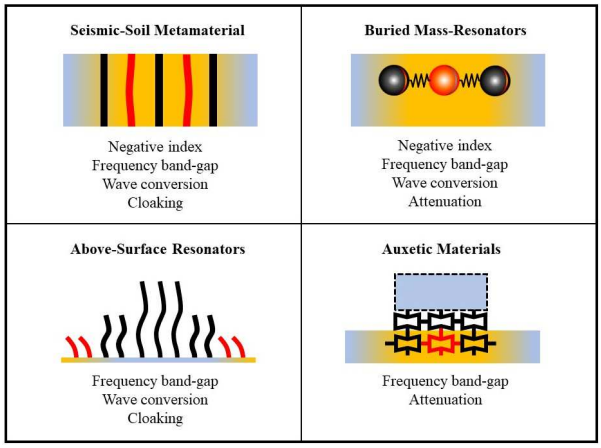

FIG 15: The four categories of seismic metamaterials.

In Fig. 15, we propose to summarize the various types of seismic metamaterials which have emerged thus far, see Section V for more details. Of course this classification is likely to evolve in the coming years. Another type of seismic metamaterial that might arise in the near future is one that would be based on analogies drawn with designs found in nature (such as in spider webs [**67**] reminiscent of mechanical lattice cloaks [**63**]) and in bio-engineering

[**42**,**68**] at the small scale, or even in archeology [**69**], see Figure 16 for comparisons between the design of an invisibility cloak for microwaves and an ancient Gallo-Roman theater, at the large scale.

Finally, if one would like to envision the future of seismic metamaterials, a rapid look at the topical subjects in photonics suggests that topological media and Parity-Time symmetry might be good candidates for next research advances. The latter is linked to non-reciprocity arising in space-time modulated media, which can be viewed as Willis media according to a homogenization model in [**70**], which starts from Eq. 1 and leads to effective equations in the form of Eq. 3-5 for a layered medium as in Figures 2 & 3.

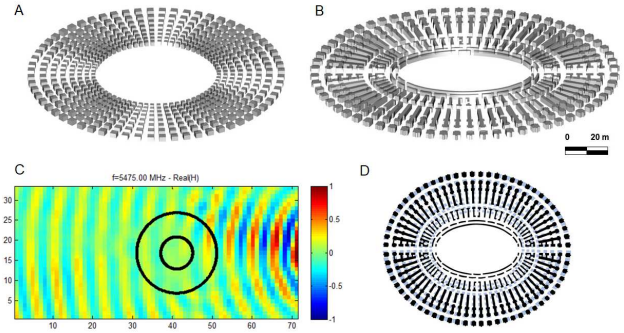

FIG. 16. Analogy between an invisibility cloak and antique Gallo-Roman theaters: (A) Schematics of an aluminium cloak 20 cm in diameter designed and tested at Institut Fresnel. (B) Schematics of a sky geophysics view extracted from a magnetic gradient map of a completely buried Gallo-Roman ex muros theater located at Autun, La Genetoye (France). Courtesy of Geocarta and G. Bossuet, in [**69**] with the permission of the authors). (C) Electric field from microwave experiment at 5.5 GHz (courtesy of R. Abdeddaim and E. Georget, Institut Fresnel) of the cloak in (A). (D) Superimposed cloak and ancient theater.

Let us finally recall that the vibration measurements on the structures must continue whether this is done under major earthquakes or as part of the measurement of seismic ambient noise [**72**]. The topic of seismic metamaterials is still in its infancy, and while research advances on the theoretical aspects of mechanical metamaterials are very promising, large scale experiments are needed to demonstrate applicability of concepts to civil engineering.

ACKNOWLEDGEMENTS

S.G. wishes to thank ERC funding (ANAMORPHISM project) during years 2011-2016 that helped strengthen collaboration between the authors. S.G. is also thankful for a visiting position in the group of Prof. R.V. Craster at Imperial College London funded by EPSRC programme grant “Mathematical fundamentals of Metamaterials for multiscale Physics and Mechanics” (EP/L024926/1).

REFERENCES

[**1**] R.D. Woods, Screening of surface waves in soils, The University of Michigan Industry Program of the College of Engineering. IP-804 (1968).
[**2**] P.K. Banerjee, S. Ahmad, K. Chen, Advanced application of BEM to wave barriers in multi-layered three-dimensional soil media, Earthquake Eng. & Structural Dynamics 16, pp. 1041–1060 (1988).
[**3**] L. Brillouin, Wave propagation in periodic structures. McGraw-Hill Book Company Inc. (1946).
[**4**] S. Brûlé, E.H. Javelaud, S. Enoch, S. Guenneau, Experiments on Seismic Metamaterials: Molding Surface Waves. Phys. Rev. Lett. 112, p. 133901 (2014).
[**5**] S. Brûlé, E.H. Javelaud, S. Enoch, S. Guenneau, Flat lens effect on seismic waves propagation in the subsoil Sci. Rep. 7 (1), p. 18066 (2017)
[**6**] M. Kadic, T. Bückmann1, R. Schittny, M. Wegener, Metamaterials beyond electromagnetism, Rep. Prog. Phys. 76, p. 126501 (2013).
[**7**] E. Yablonovitch, Inhibited spontaneous emission in solid-state physics and electronics, Phys. Rev. Lett. 58, p. 2059 (1987).
[**8**] S. John, Strong localization of photons in certain disordered dielectric superlattices, Phys. Rev. Lett. 58, pp. 2486–2489 (1987).
[**9**] K. Srinivasan, O. Painter, Momentum space design of high-q photonic crystal optical cavities, Opt. Express 10, pp. 670–684 (2002).
[**10**] R. Zengerle, Light propagation in singly and doubly periodic waveguides, J. Mod. Opt. 34, pp. 1589–1617 (1987).
[**11**] M. Notomi, Theory of light propagation in strongly modulated photonic crystals: Refractionlike behaviour in the vicinity of the photonic band gap, Phys. Rev. B 62, pp. 10696–10705 (2000).
[**12**] B. Gralak, S. Enoch, G. Tayeb, Anomalous refractive properties of photonic crystals, J. Opt. Soc. Am. A 17, pp. 1012–1020 (2000).
[**13**] C. Luo, S.G. Johnson, J.D. Joannopoulos, J.B. Pendry, Allangle negative refraction without negative effective index, Phys. Rev. B 65, p. 201104 (2002).
[**14**] Veselago, V.G. (1968). The electrodnamics of substances with simultaneously negative values of ε and μ, Soviet Physics Uspekhi 10(4), pp. 509–514.
[**15**] J.B. Pendry, A.J. Holden, D.J. Robbins, W.J. Stewart, Magnetism from conductors and enhanced nonlinear phenomena, IEEE Transactions on Microwave Theory and Techniques 47(11), p. 2075 (1999).
[**16**] D.R. Smith, W.J. Padilla, V.C. Vier, S.C. Nemat-Nasser, S. Schultz, Phys. Rev. Lett. 84, p. 4184 (2000).

[**17**] J.B. Pendry, Negative refraction makes a perfect lens, Phys. Rev. Lett. 85, pp. 3966–3969 (2000).
[**18**] G. Dolling, C. Enkrich, M. Wegener, C.M. Soukoulis, S. Linden, Observation of simultaneous negative phase and group velocity of light, Science 312, p. 892 (2006).
[**19**] D. Schurig, J.J. Mock, B.J. Justice, S.A. Cummer, J.B. Pendry, A.F. Starr, D.R. Smith, Metamaterial electromagnetic cloak at microwave frequencies, Science 314(5801), pp. 977–980 (2006).
[**20**] A. Alù, M. Silveirinha, A. Salandrino, E.N. Engheta, Epsilonnear-zero metamaterials and electromagnetic sources: Tailoring the radiation phase pattern, Phys. Rev. B 75, p. 155410 (2007).
[**21**] S. Enoch, G. Tayeb, P. Sabouroux, N. Guérin, P. Vincent, A metamaterial for directive emission, Phys. Rev. Lett. 89, p. 213902 (2002).
[**22**] T. Antonakakis, R.V. Craster, High frequency asymptotics for microstructured thin elastic plates and platonics, Proc. R. Soc. Lond. A 468, p. 1408 (2012).
[**23**] M. Dubois, E. Bossy, S. Enoch, S. Guenneau, G. Lerosey, P. Sebbah, Time drive super oscillations with negative refraction, arXiv:1303.3022v2 (2013).
[**24**] R. Martinez-Sala, J. Sancho, J.V. Sanchez, V. Gomez, J. Llinares, F. Meseguer, Nature 378, p. 241 (1995).
[**25**] A. Sukhovich, B. Merheb, K. Muralidharan, J.O. Vasseur, Y. Pennec, P.A. Deymier, J.H. Page, Experimental and theoretical evidence for subwavelength imaging in phononic crystals, Phys. Rev. Lett. 102, p. 154301 (2009).
[**26**] Z. Liu, X. Zhang, Y. Mao, Y. Zhu, Z. Yang, C.T. Chan, P. Sheng, Locally resonant sonic materials, Science 289, p. 1734 (2000).
[**27**] N. Fang, D. Xi, J. Xu, M. Ambati, W. Srituravanich, C. Sun, X. Zhang, Nat. Mater. **5**, p. 452 (2006).
[**28**] J. Christensen, F.J. Garcia De Abajo, Anisotropic metamaterials for full control of acoustic waves, Phys. Rev. Lett. 108, p. 124301 (2012).
[**29**] R. Craster, S. Guenneau, Acoustic Metamaterials: Negative Refraction, Imaging, Lensing and Cloaking, vol. 166, R. Craster and S. Guenneau, Eds. Springer Verlag (2013).
[**30**] G.W. Milton, M. Briane, J.R. Willis, On cloaking for elasticity and physical equations with a transformation invariant form, New J. Phys. 8, p. 248 (2006).
[**31**] M. Brun, S. Guenneau, A.B. Movchan, Achieving control of in-plane elastic waves, Appl. Phys. Lett. 94, p. 061903 (2009).
[**32**] A. Norris, A.L. Shuvalov, Elastic cloaking theory, Wave Motion, 48(6), pp. 525–538 (2011).
[**33**] M. Farhat, S. Guenneau, S. Enoch, Broadband cloaking of bending waves via homogenization of multiply perforated radially symmetric and isotropic thin elastic plates, Phys. Rev. B 85, p. 020301 R (2012).
[**34**] J. Huang, W. Liu, Z. Shi, Surface-wave attenuation zone of layered periodic structures and feasible application in ground vibration reduction. Constr. Build. Mater. 141, pp. 1-11 (2017).
[**35**] M.S. Kushwaha, P. Halevi, G. Martinez, L. Dobrzynski, B. Djafari-Rouhani, Theory of acoustic band structure of periodic elastic composites, Phys. Rev. B 49, pp. 2313–2322 (1994).
[**36**] S. Brûlé, F. Cuira. Practice of soil-structure interaction under seismic loading. AFNOR Edition (2017).
[**37**] S. Brûlé, B. Ungureanu, Y. Achaoui, A. Diatta, R. Aznavourian, T. Antonakakis, R.V. Craster, S. Enoch, S. Guenneau, 2017. Metamaterial-like Transformed Urbanism. Innov. Infrastruct. Solut. 2, p. 20 (2017).
[**38**] S. Brûlé, S. Duquesnoy, Change of ground type by means of dynamic compaction: Consequences on the calculation of seismic loadings Innov. Infrastruct. Solut. 1, p. 39 (2016).
[**39**] J.B. Pendry, D. Schurig, D.R. Smith, Controlling Electromagnetic Fields. Science 312 (5781), pp. 1780–1782 (2006).
[**40**] S. Brûlé, E. Javelaud, S. Guenneau, S. Enoch, D. Komatitsch, Seismic metamaterials. Proceedings of the 9th International Conference of the Association for Electrical, Transport and Optical Properties of Inhomogeneous Media in Marseille, France (2012).
[**41**] Y. Achaoui, T. Antonakakis, S. Brûlé, R.V. Craster, S. Enoch, S. Guenneau, Clamped seismic metamaterials: Ultra-Low Broad Frequency stop-bands. New J. Phys. (19), p. 063022 (2017).
[**42**] R. Aznavourian, T. Puvirajesinghe, S. Brûlé, S. Enoch, S. Guenneau, Spanning the scales of mechanical metamaterials using time domain simulations in transformed crystals, graphene flakes and structured soils. J. Phys.: Condens. Matter. 29(43), p. 433004 (2017).
[**43**] A. Diatta, Y. Achaoui, S. Brûlé, S. Enoch, S. Guenneau, Control of Rayleigh-like waves in thick plate Willis metamaterials. AIP Advances 6, p. 121707 (2016).
[**44**] G.W. Milton, J.R. Willis, On modifications of Newton's second law and linear continuum elastodynamics. Proceedings of the royal society of london A: Mathematical, Physical and Engineering Sciences 463, pp. 855-880 (2007).
[**45**] S. Brûlé, S. Enoch, S. Guenneau, Sols structurés sous sollicitation dynamique : des métamatériaux en géotechnique, Rev. Fr. Geotech. 151, p. 4 (2017).
[**46**] M. Miniaci, A. Krushynska, F. Bosia, N.M. Pugno, Large scale mechanical metamaterials as seismic shields. New J. Phys. 18, p. 083041 (2016).
[**47**] S. Krödel, N. Thome, C. Daraio, Wide band-gap seismic metastructures. Ex. Mech. Letters 4, pp. 111-117 (2015).
[**48**] Y. Achaoui, B. Ungureanu, S. Enoch, S. Brûlé, S. Guenneau, Seismic waves damping with arrays of inertial resonators. Ex. Mech. Letters 8, pp. 30-38 (2016).

[**49**] G. Finocchio, O. Casablanca, G. Ricciardi, U. Alibrandi, F. Garescì, M. Chiappini, B. Azzerboni, Seismic metamaterials based on isochronous mechanical oscillators. Appl. Phys. Lett. 104, p. 191903 (2014).

[**50**] A. Colombi, P. Roux, S. Guenneau, P. Gueguen, R.V. Craster, Forests as a natural seismic metamaterial: Rayleigh wave bandgaps induced by local resonances. Sci. Rep. 6, p. 19238 (2016).

[**51**] A. Colombi, D. Colquitt, P. Roux, S. Guenneau, R.V. Craster, A seismic metamaterial: the resonant metawedge. Sci. Rep. 6, p. 27717 (2016).

[**52**] A. Maurel, J.J. Marigo, K. Pham, S. Guenneau, Conversion of Love waves in a forest of trees, Phys. Rev. B 98 (13), p. 134311 (2018).

[**53**] F. Zolla, G. Bouchitté, S. Guenneau, Pure currents in foliated waveguides, The Quarterly Journal of Mechanics & Applied Mathematics 61 (4), pp. 453-474 (2008).

[**54**] A Palermo, A Marzani, Control of Love waves by resonant metasurfaces, Sci. Rep. 8(1), p. 7234 (2018).

[**55**] A. Wirgin, Computational parameter retrieval approach to the dynamic homogenization of a periodic array of rigid rectangular blocks, arXiv:1803.04717v1 (2018).

[**56**] G. Carta, I.S. Jones, N.V. Movchan, A.B. Movchan, M.J. Nieves, Gyro-elastic beams for the vibration reduction of long flexural systems. Proc. R. Soc. A 473, p. 20170136 (2017).

[**57**] H.L Wong, M.D. Trifunac, B. Westermo, Effects of surface and subsurface irregularities on the amplitude of monochromatic waves. Bull. Seismol. Soc. Am. 67, pp. 353–368 (1977).

[**58**] A. Wirgin, P-Y. Bard, Effects of buildings on the duration and amplitude of ground motion in Mexico City. Bull. Seismol. Soc. Am. 86(3), pp. 914–920 (1996).

[**59**] Ph. Guéguen, P-Y. Bard, F.J. Chavez-Garcia, Site-city seismic interaction in Mexico City-like environments: an analytical study. Bull. Seismol. Soc. Am. 92(2), pp. 794–811 (2002).

[**60**] C. Boutin, P. Roussillon, Assessment of the urbanization effect on seismic response. Bull. Seismol. Soc. Am. 94(1), pp. 251–268 (2004).

[**61**] B. Ungureanu, Y. Achaoui, S. Enoch, S. Brûlé, S. Guenneau, Auxetic-like metamaterials as novel earthquake protections. EPJ Appl. Metamat. 2015(2), p. 17 (2016).

[**62**] L. d'Alessandro, V. Zega, R. Ardito, A. Corigliano, 3D auxetic single material periodic structure with ultra-wide tunable bandgap Sci. Reports 8, p. 2262 (2018).

[**63**] T. Buckmann, M. Kadic, R. Schittny, M. Wegener, Mechanical cloak design by direct lattice transformation Proceedings of the National Academy of Sciences 112(16), pp. 4930-4934 (2015).

[**64**] O. Casablanca, G. Ventura, F. Garescì, B. Azzerboni, B. Chiaia, M. Chiappini, and G. Finocchio, Seismic isolation of buildings using composite foundations based on metamaterials. J. Appl. Phys. 123, p. 174903 (2018).

[**65**] H.J. Xiang, Z.F. Shi, S.J. Wang, Y.L. Mo, Periodic materials-based vibration attenuation in layered foundations: experimental validation. Smart Mater. Struct. 21, p. 112003 (2012).

[**66**] M. Brun, G.F. Giaccu, A.B. Movchan, N.V. Movchan, Asymptotics of eigenfrequencies in the dynamic response of elongated multi-structures, Proc. of the Roy. Soc. Lond. A 468 (2138), 378-394 (2011).

[**67**] G. Greco, M. F. Pantano, B. Mazzolai, N. Pugno, Imaging and mechanical characterization of different junctions in spider orb webs, Sci. Rep. 9, p. 5776 (2019)

[**68**] J. Zang, S. Ryu, N. Pugno, Q. Wang, Q. Tu, M.J. Buehler, X. Zhao, Multifunctionality and control of the crumpling and unfolding of large-area graphene, Nature materials 12 (4), p. 321 (2015).

[**69**] G. Bossuet, A. Louis, F. Ferreira, Y. Labaune, C. Laplaige, Le sanctuaire suburbain de la Genetoye à Autun/Augustodunum (Saône-et-Loire). Apport de l'approche combinée de données spatialisées à la restitution du théâtre antique du Haut du Verger, Gallia, 72-2, pp. 205-223 (2015).

[**70**] H. Nassar, X.C. Xu, A.N. Norris, G.L. Huang, Modulated phononic crystals: Non-reciprocal wave propagation and Willis materials, Journal of the Mechanics and Physics of Solids 101, pp. 10-29 (2017).

[**71**] U. Leonhardt, Optical conformal mapping, Science 312, pp. 1777-1780 (2006).

[**72**] Report of the French Association for Earthquake Engineering (AFPS) on the Mexico Earthquake of September 19, 2017 (http://www.afps-seisme.org/SEISMES/Missions-post-sismiques/Actualites-des-missions-post-sismiques*)*